AD-A037 899 BALLISTIC RESEARCH LABS ABERDEEN PROVING GROUND MD F/G 20/13
CONTINUOUS SURFACE-DENSITY MONTE CARLO SOLUTION TO THE DIRICHLE--ETC(U)
MAR 77 N E BANKS, T J HOFFMAN

UNCLASSIFIED BRL-1966 NL

| OF |
AD
A037899

END

DATE
FILMED
4-77

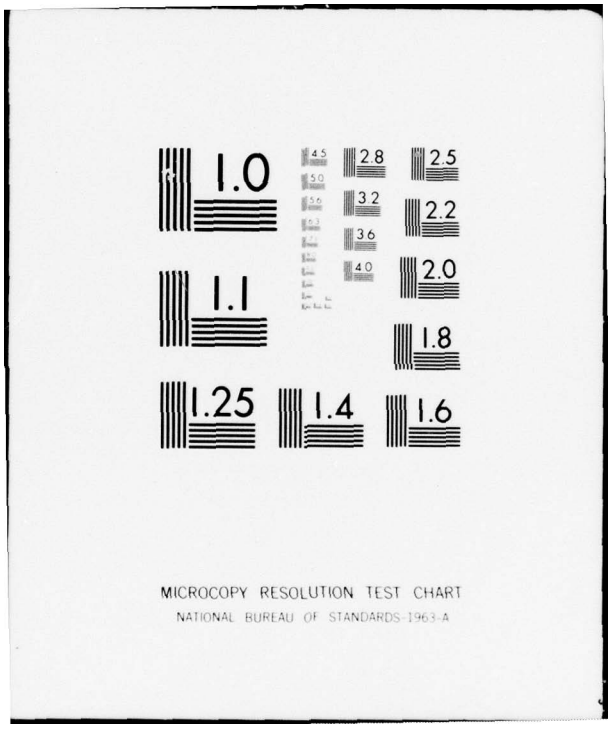
1.0
1.1
1.25
1.4
1.6
1.8
2.0
2.2
2.5
2.8
3.2
3.6
4.0
4.5
5.0
5.6
6.3
MICROCOPY RESOLUTION TEST CHART
NATIONAL BUREAU OF STANDARDS-1963-A

BRL

AD

REPORT NO. 1966

CONTINUOUS SURFACE-DENSITY MONTE CARLO SOLUTION TO THE DIRICHLET HEAT-TRANSFER PROBLEM

Norman E. Banks
Thomas J. Hoffman

March 1977

USA BALLISTIC RESEARCH LABORATORY
ABERDEEN PROVING GROUND, MARYLAND

Destroy this report when it is no longer needed.
Do not return it to the originator.

Secondary distribution of this report by originating or sponsoring activity is prohibited.

Additional copies of this report may be obtained from the National Technical Information Service, U.S. Department of Commerce, Springfield, Virginia 22151.

The findings in this report are not to be construed as an official Department of the Army position, unless so designated by other authorized documents.

UNCLASSIFIED

SECURITY CLASSIFICATION OF THIS PAGE (When Data Entered)

REPORT DOCUMENTATION PAGE	READ INSTRUCTIONS BEFORE COMPLETING FORM
1. REPORT NUMBER: BRL [illegible] NO. 1966	2. GOVT ACCESSION NO. / 3. RECIPIENT'S CATALOG NUMBER
4. TITLE (and Subtitle): CONTINUOUS SURFACE-DENSITY MONTE CARLO SOLUTION TO THE DIRICHLET HEAT-TRANSFER PROBLEM.	5. TYPE OF REPORT & PERIOD COVERED: Final rept.
	6. PERFORMING ORG. REPORT NUMBER
7. AUTHOR(s): Norman E. Banks, Ballistic Research Laboratory Thomas J. Hoffman, Science Applications, Inc.	8. CONTRACT OR GRANT NUMBER(s)
9. PERFORMING ORGANIZATION NAME AND ADDRESS: US Army Ballistic Research Laboratory Aberdeen Proving Ground, Maryland 21005	10. PROGRAM ELEMENT, PROJECT, TASK AREA & WORK UNIT NUMBERS: RDT&E 1L161102AH43
11. CONTROLLING OFFICE NAME AND ADDRESS: US Army Materiel Development & Readiness Command 5001 Eisenhower Avenue Alexandria, Virginia 22333	12. REPORT DATE: MARCH 1977 13. NUMBER OF PAGES: 29
14. MONITORING AGENCY NAME & ADDRESS (if different from Controlling Office): 29 p.	15. SECURITY CLASS. (of this report): Unclassified 15a. DECLASSIFICATION/DOWNGRADING SCHEDULE

16. DISTRIBUTION STATEMENT (of this Report)

Approved for public release; distribution unlimited.

17. DISTRIBUTION STATEMENT (of the abstract entered in Block 20, if different from Report)

18. SUPPLEMENTARY NOTES

19. KEY WORDS (Continue on reverse side if necessary and identify by block number)

Continuous Monte Carlo, Heat Transfer, Surface Density, Integral Equations

20. ABSTRACT (Continue on reverse side if necessary and identify by block number) (as)

In this report a new and efficient Monte Carlo approach to the solution of the Dirichlet problem is developed and implemented. This approach, the surface-density technique, is capable of treating problems with arbitrary geometric complexity. No compromises with the physics of the problem are required, and new insight into efficient Monte Carlo solutions of many difficult problems of mathematical physics is gained. The adaptability of Monte Carlo radiation transport codes to this method is highly useful for → next page

DD FORM 1 JAN 73 1473 EDITION OF 1 NOV 65 IS OBSOLETE

UNCLASSIFIED 050 750

SECURITY CLASSIFICATION OF THIS PAGE (When Data Entered)

20. ABSTRACT (Continued)

problems that require calculation of both heat transfer and radiation transport, e.g., analyses of fuel-shipping-casks. Criticality, shielding, and heat transfer can be calculated with one geometric description and one computer code.

TABLE OF CONTENTS

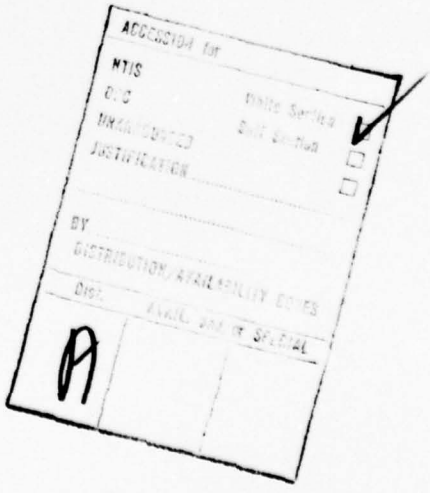

LIST OF FIGURES

LIST OF TABLES

1. INTRODUCTION

In radiation transport theory, Monte Carlo techniques have been developed that reproduce the physical model in as much detail as is necessary. As such, these approaches provide a powerful tool in the solution of complex, neutron and gamma-ray transport problems. However, applications outside the area of radiation transport have been discouraging. In the past, brute-force stochastic approaches have been attempted in the solutions of finite difference equations. The extravagant costs of development and computation of such approaches have maligned Monte Carlo techniques in general. More recently[1], the use of modified Green's functions has produced an efficient Monte Carlo method for solving complex three-dimensional time-dependent parabolic and elliptic partial differential equations.

This paper reports a new Monte Carlo approach to the Dirichlet problem[2,3,4]. This approach, which simulates a surface-density equation, can treat problems with arbitrary, geometric complexity. It requires no compromises with the physics of the problem and provides a new insight into efficient Monte Carlo solutions of many difficult problems of mathematical physics. For the sake of clarity, the terminology of heat transfer will be used, but this surface-density approach is also applicable to fluid flow, stress analysis, and many other problems in physics and engineering.

---

1. E.S. Troubetzkoy et al., "Solution of Time Dependent Diffusion Equation in Complex Geometry by the Monte Carlo Method", BRL Interim Technical Report, MAGI 7053 (Rough Draft) 1975.

2. T.J. Hoffman and N.E. Banks, "Monte Carlo Solution to the Dirichlet Problem with the Double Layer Potential Density", Trans. Am. Nucl. Soc., 18, 136, (1974).

3. N.E. Banks and T.J. Hoffman, "Continuous Monte Carlo Solution to the Dirichlet Heat Transfer Problem Using the Double Layer Potential", 20th Army Mathematics Conference, Boston, MA (1974).

4. T.J. Hoffman and N.E. Banks, "Monte Carlo Solution to the Dirichlet Problem", Transactions of the ANL-NEACRP International Meeting on Monte Carlo Applications, Argonne National Laboratory, July 1-3, 1974.

Section 2 describes the mathematical bases of the approach and presents a comprehensive review of previous Monte Carlo approaches. Section 3 develops and illustrates the concept of the surface-density technique. The mathematical development involves manipulation of the integral equation for the density of the potential of a double layer. Since the mathematical justification for this approach is intricate, a pictorial illustration will be presented to aid computer implementation. Section 4 demonstrates the method by application to three heat-transfer problems of varying degrees of geometric complexity. The final section presents the conclusions of this work and recommendations for further study.

2. BACKGROUND

2.1 Problem Statement.

The Dirichlet problem is an old problem of mathematics that frequently arises in physical applications. The problem is to find a function, $T(\bar{r})$, that is harmonic in a given region R, i.e.,

$$\nabla^2 T(\bar{r}) = 0.0 \text{ in } R \tag{1}$$

and assumes prescribed values on the boundary, S, enclosing R, i.e.,

$$T(\bar{r}) \rightarrow \phi(\bar{r}_s) \text{ on } S. \tag{2}$$

From a heat-transfer point of view, the problem is to find the steady-state temperature, T, at a point $\bar{r}$ within a homogeneous region, given the surface temperature, ϕ.

There are many ways to solve this problem - both deterministic and stochastic. Examples of deterministic methods are finite difference, finite element, Fourier analysis, and Green's functions. These methods will not be discussed here. Instead we shall describe the stochastic, or Monte Carlo, approaches to the solution of the Dirichlet problem. For the sake of clarity these approaches will be illustrated for two-dimensional regions, but all are applicable to three-dimensional problems.

2.2 Discrete Monte Carlo Approach.

Perhaps the most widely used Monte Carlo approach to the Dirichlet problem divides the region, R, with a grid as shown in Figure 1 (see Curtiss (5) for a literature review). The temperature at each

5. J.H. Curtiss, "Sampling Methods Applied to Differential and Difference Equations", Seminar on Scientific Computation, International Business Machines Corporation (1949).

node of a uniform grid is the average of the temperatures at the four adjacent nodes. The Monte Carlo random walk consists of starting a "walk" at the point where the temperature is desired, i.e., $\bar{r}$ in Figure 1. With equal probability* one of the four adjacent nodes (indicated by "X's" in Figure 1) is selected, and the walker moves to this new node. The temperature at the selected node is the contribution to the temperature at $\bar{r}$.

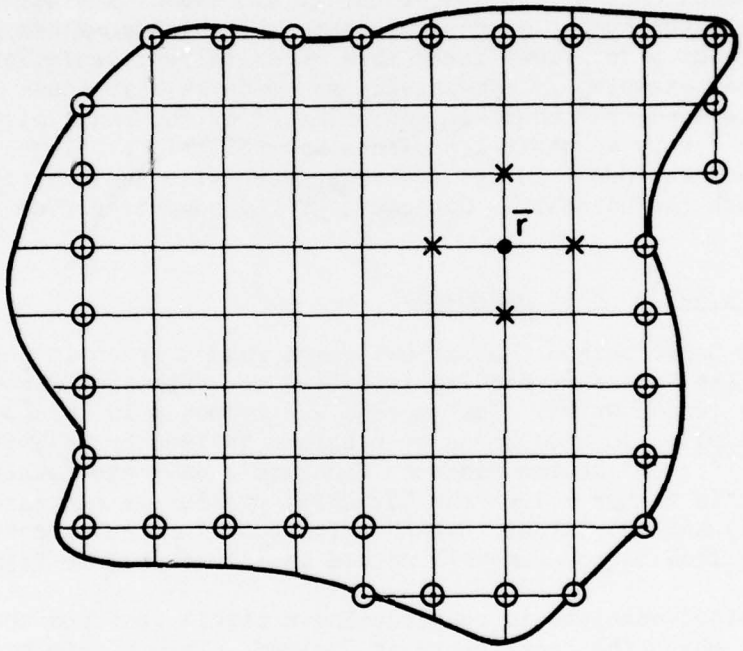

Figure 1. Discrete Monte Carlo Approach to the Dirichlet Problem.

Since the temperature at the new node is not known, the random-selection technique is iterated until the walker arrives at a point where the temperature is known, i.e., a boundary point (see Equation (2)). When the walker encounters one of the circled nodes which approximate the

* The mesh size need not be constant throughout the grid; it was done here for the purpose of illustration. If the grid is not uniform, the probability of the walker moving to each of the adjacent nodes is no longer 1/4.

boundary, this boundary temperature is saved as a contribution to the temperature at $\bar{r}$. Then a new walk (history) is initiated at $\bar{r}$, and the process is repeated. The average of these saved boundary temperatures from many histories is a Monte Carlo estimate of the desired temperature at $\bar{r}$.

With this method, often referred to as the "drunkard's walk", the walker is restricted to move only in the four, specified directions from any given point. Therefore, only the finite-difference approximation to the problem is obtained, so that the accuracy of this discrete approach depends on the fineness of the grid. Use of a finer grid not only increases the number of possible paths by which a walker can reach the surface, but also allows for a more accurate representation of the boundary. For example, if a mesh size as crude as that shown in Figure 1 were used, the boundary approximated by the small circles would not be a very accurate representation of this problem. Of course a finer grid structure requires a smaller step size and therefore more steps to reach the boundary. Consequently the computing time will be longer.

2.3 Floating Random-Walk Approach.

A Monte Carlo method that allows large random steps in the solution to the Dirichlet problem is called the "spherical process" or "floating random walk". This method was proposed in 1956 by Brown[6] and applied to heat transfer problems in 1965 by Haji-Sheikh and Sparrow[7,8]. Unlike the discrete drunkard's walk previously described, this method solves the Dirichlet problem as expressed in Equations (1) and (2) rather than the finite-difference approximation to it. This floating random-walk method is illustrated in Figure 2.

This method consists in constructing a circle centered about the point, $\bar{r}$, at which the temperature is desired. This circle must lie entirely within the region, R, and, for efficiency, should be tangent to the nearest boundary point from $\bar{r}$ as shown in Figure 2. The first step in this process is the random, uniform selection of a point on the circumference of this circle, say at position $\bar{r}_1$. Another circle,

---

6. G.M. Brown, "Monte Carlo Methods", Modern Mathematics for the Engineer, McGraw-Hill Book Co., Inc., New York, NY (1956).

7. A. Haji-Sheikh and E.M. Sparrow, "The Solution of Heat Conduction Problems by Probability Methods", J. Heat Transfer, ASME, 89 (1967).

8. A. Haji-Sheikh and E.M. Sparrow, "The Floating Random Walk and Its Application to Monte Carlo Solutions of Heat Equations", J. SIAM, Appl. Math., 14, (1966).

centered at $\bar{r}_1$ and tangent to the nearest point on the surface, is then constructed. A point is randomly selected on this circumference, e.g., $\bar{r}_2$, and the walker is moved to this point. The walk continues until it encounters the surface, and the surface temperature at the point of encounter is saved. A Monte Carlo estimate of the temperature at the point $\bar{r}$ is the average of many such random walks. Of course, the surface is never really encountered, because the probability of selecting the tangency point is zero. This problem is circumvented by defining a thin layer inside the boundary, indicated by the dashed line in Figure 2. When the walker enters this layer, he is assumed to be at the boundary.

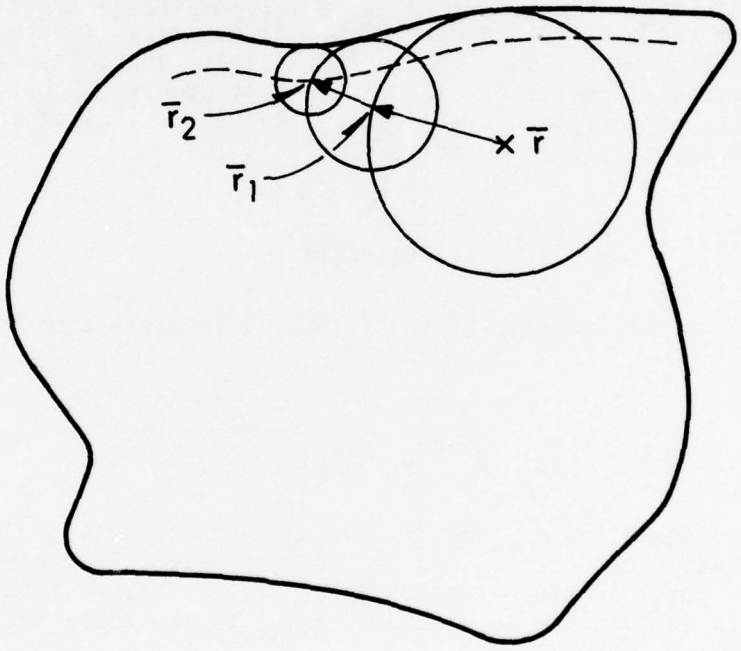

Figure 2. Floating Random-Walk Approach to the Dirichlet Problem.

The floating random walk allows large random steps for points far removed from the boundary, but as the walker approaches the boundary, smaller steps are taken. For complex geometries, however, considerable computer time is required to locate the nearest boundary point from the current walker position in order to construct the circle. The artificial boundary layer required for convergence also introduces an approximation, or error, into the calculation. If it is too large, the wrong problem is solved; if it is too small, the computing time is extravagant. The error approaches zero as the thickness of the layer approaches zero; however, the computation time approaches infinity.

Shapes other than circles have been proposed in an attempt to better fit the boundary[9]. A floating random-walk technique using rectangles (rectangular parallelepipeds for three-dimensional problems) is under development[10]. This approach has proved very useful for nonlinear problems and has been shown to be very efficient in geometries whose physical boundaries are rectangular.

3. THE MONTE CARLO SURFACE-DENSITY TECHNIQUE

3.1 Mathematical Development.

Unlike the Monte Carlo approaches previously described, the surface density approach requires no artificial boundaries or geometry searches for the closest boundary point, allows large random steps, and is a continuous method. The surface-density approach transforms the differential formulation of the Dirichlet problem, Equations (1) and (2), into an integral formulation using the density of the potential of a double layer, $\mu(\bar{r}_s)$, as follows:[11,12]

$$T(\bar{r}) = \int_S d\bar{r}_s \, \mu(\bar{r}_s) \frac{(\bar{r}-\bar{r}_s)\cdot\hat{n}_s}{4\pi|\bar{r}-\bar{r}_s|^3} \tag{3}$$

where $\mu(\bar{r}_s)$ *is the solution of the following integral equation,*

$$\mu(\bar{r}_s) = 2\phi(\bar{r}_s) + \frac{1}{2\pi} \int_S d\bar{r}_p \, \mu(\bar{r}_p) \frac{(\bar{r}_p-\bar{r}_s)\cdot\hat{n}_p}{|\bar{r}_p-\bar{r}_s|^3} \, . \tag{4}$$

In the above equations $d\bar{r}_s$ and $d\bar{r}_p$ are surface elements about the surface position vectors $\bar{r}_s$ and $\bar{r}_p$ respectively. The symbol $\hat{n}_p$ denotes the unit, inward-directed vector that is normal to S at $\bar{r}_p$. $T(\bar{r})$ is the desired temperature; $\phi(\bar{r}_s)$ is the known surface temperature.

---

9. M.E. Muller, "Some Continuous Monte Carlo Methods for the Dirichlet Problem", Annals of Math. Statistics, 27, (1956).

10. M.H. Kalos and H. Steinberg, private communications at the ANL-NEACRP International Meeting on Monte Carlo Applications, Argonne National Laboratory, July 1-3, 1974.

11. S.G. Mikhlin, Linear Integral Equations, Hindustan Publishing Corporation, Delhi, India (1960).

12. W.V. Lovitt, Linear Integral Equations, Dover Publications, Inc., New York, NY (1950).

The notation can be simplified by writing Equations (3) and (4) as:

$$\mu(\bar{r}_s) = Q(\bar{r}_s) + \int d\bar{r}_p \; \mu(\bar{r}_p) \; K(\bar{r}_p,\bar{r}_s) \tag{5}$$

and

$$T(\bar{r}) = \int d\bar{r}_s \; \mu(\bar{r}_s) R(\bar{r},\bar{r}_s), \tag{6}$$

where the definitions of $Q(\bar{r}_s)$, $K(\bar{r}_p,\bar{r}_s)$ and $R(\bar{r},\bar{r}_s)$ follow directly from Equations (3) and (4).

The reformulated problem, Equations (5) and (6) may appear more complex than the original problem, Equations (1) and (2). The motivation for this reformulation, or integral transformation, is that similar kinds of equations are solved in Monte Carlo radiation transport. The equation that is normally solved in Monte Carlo radiation transport is called the emergent-particle-density equation[13]. It is a Fredholm integral equation of the second kind. Equation (5) for $\mu(\bar{r}_s)$ is also a Fredholm integral equation of the second kind. Stochastic algorithms have been devised for solving this type of equation[14,15].

Consider the following particle transport analogy:

1. λ(register for the quantity of interest) is set to 0.0.

2. $Q(\bar{r}_s)d\bar{r}_s$ is the probability that an initial event will occur in $d\bar{r}_s$ about $\bar{r}_s$. $Q(\bar{r}_s)$ is assumed to be a normalized, probability distribution function (p.d.f.). Therefore, on the boundary of the region an initial event site, $\bar{r}_{so}$, is selected from the given function $2\phi(\bar{r}_s)$. The quantity $R(\bar{r},\bar{r}_{so})$ is added to λ.

3. $K(\bar{r}_p,\bar{r}_s)d\bar{r}_s$ is the probability that an event at $\bar{r}_p$ will be followed by an event in $d\bar{r}_s$ about $\bar{r}_s$. Therefore, another event will occur with probability $K(\bar{r}_{so},\bar{r}_s)d\bar{r}_s = \sigma$.

---

13. T.W. Armstrong and P.N. Stevens, "A V^o Importance Function for the Monte Carlo Calculation of the Deep Penetration of Gamma Rays", Pergamon Press, New York, NY (1969).

14. H. Kahn, "Applications of Monte Carlo", Part II, AECU-3259, Rand Corporation, Santa Monica, CA (1956).

15. R.R. Coveyou, V.R. Cain and K.J. Yost, "Adjoint and Importance in Monte Carlo Applications", NSE, 27 (1967).

The site, $\bar{r}_{s1}$, of the next event is selected from the p.d.f.

$\frac{1}{\sigma} K(\bar{r}_{so},\bar{r}_s)$. The quantity $R(\bar{r},\bar{r}_{s1})$ is added to λ.

4. Step 3 is repeated until the particle fails to survive an event (probability = $1-\sigma$).

5. When the particle is killed, the site of another source event is selected from $Q(\bar{r}_s)$. This process is repeated many times, say m.

6. A Monte Carlo estimate of $T(\bar{r})$ is λ/m.

Two major drawbacks soon appear when the above procedure is attempted with Equations (5) and (6):

1. Sampling from the distributions in Equation (5) is extremely difficult. Except for very simple regions,

   selection from $\frac{1}{\sigma} K(\bar{r}_p,\bar{r}_s)$ is virtually impossible.

2. The Neumann series to approximate a solution of Equation (5) (i.e., tallying the contribution at each event as described in the particle transport analogy) diverges[12].

The first of these difficulties can be circumvented with a formulation adjoint to that of Equations (5) and (6), i.e.,

$$T(\bar{r}) = \int d\bar{r}_s \; Q(\bar{r}_s) \; \mu^*(\bar{r}_s), \tag{7}$$

$$\mu^*(\bar{r}_s) = R(\bar{r},\bar{r}_s) + \int K(\bar{r}_s,\bar{r}_p)\mu^*(\bar{r}_p)d\bar{r}_p. \tag{8}$$

With Equation (8) initial events are selected from $R(\bar{r},\bar{r}_s)$, i.e., the probability of the first event occurring in the surface element $d\bar{r}_s$ is

$$p(\bar{r}_s)d\bar{r}_s = \frac{(\bar{r} - \bar{r}_s)\cdot\hat{n}_s}{4\pi|\bar{r}-\bar{r}_s|^3} \; d\bar{r}_s \; . \tag{9}$$

Equation (9) is a p.d.f. for convex regions. We define, for brevity, a convex region as a region comprised of a convex set of points. The solid angle subtended by the surface element $d\bar{r}_s$ when viewed from $\bar{r}$

is, by definition[16],

$$d\bar{\Omega} = \frac{(\bar{r}-\bar{r}_s)\cdot\hat{n}_s}{|\bar{r}-\bar{r}_s|^3}\, d\bar{r}_s \ . \tag{10}$$

Since, for convex regions, the probability of an initial event in solid angle $d\bar{\Omega}$ about the direction $\bar{\Omega}$ must equal the probability of the initial event in $d\bar{r}_s$ about $\bar{r}_s$,

$$p(\bar{\Omega})d\bar{\Omega} = p(\bar{r}_s)d\bar{r}_s . \tag{11}$$

Substitution of Equations (9) and (10) into Equation (11) gives

$$p(\bar{\Omega}) = \frac{1}{4\pi} \ . \tag{12}$$

Consequently, the site of the initial event can be determined by selecting an isotropic direction from $\bar{r}$. The point where this trajectory strikes the surface is $\bar{r}_{so}$.

Equation (8) makes the selection of subsequent event sites as simple as the selection of initial sites. If an event occurs at $\bar{r}_{so}$ the site, $\bar{r}_{s1}$, of the next event, can be selected from*

$$|K(\bar{r}_{s1},\bar{r}_{so})|d\bar{r}_{s1} = \frac{(\bar{r}_{so} - \bar{r}_{s1})\cdot\hat{n}_{s1}}{2\pi|\bar{r}_{so} - \bar{r}_{s1}|^3}\, d\bar{r}_{s1} \ . \tag{13}$$

The right-hand side (RHS) of Equation (13) is just $\frac{1}{2\pi}$ times the solid angle subtended by $d\bar{r}_{s1}$ as viewed from $\bar{r}_{so}$. Therefore, subsequent sites can be obtained by selecting an isotropic direction into the region from $\bar{r}_{so}$. The point where a ray in this direction intersects the surface is $\bar{r}_{s1}$. Note that the function in Equation (13) is a p.d.f. because the total solid angle subtended by the surface from a point on the surface is 2π for convex regions.

---

16. W. Kaplan, Advanced Calculus, Addison-Wesley Publishing Co., Inc. Reading, MA (1959).

* A statistical weight adjustment $\left(\frac{K(\bar{r}_s,\bar{r}_p)}{|K(\bar{r}_s,\bar{r}_p)|} = -1\right)$ is also required when selection of subsequent events is made with Equation (13).

The above treatment of the selection of initial and subsequent event sites is valid only for regions that are convex. However, even if the region of interest is not convex, Equation (9) is a properly normalized distribution function. Figure 3 illustrates this point.

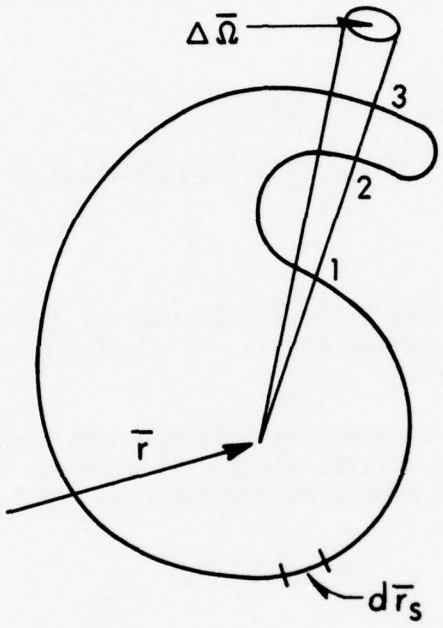

Figure 3. Selection of Initial Event Site Using Solid Angle.

The probability of selecting $\bar{r}_{so}$ on the surface element labeled "1" is $p_1 = \frac{\Delta\bar{\Omega}}{4\pi}$; the "probability" for surface element 2 is $-\frac{\Delta\bar{\Omega}}{4\pi}$; and the probability for surface element 3 is $\frac{\Delta\bar{\Omega}}{4\pi}$. The total probability for the selection of $\bar{r}_{so}$ in $\Delta\bar{\Omega}$ is

$$P_1 + P_2 + P_3 = \frac{\Delta\bar{\Omega}}{4\pi} - \frac{\Delta\bar{\Omega}}{4\pi} + \frac{\Delta\bar{\Omega}}{4\pi} = \frac{\Delta\bar{\Omega}}{4\pi} . \qquad (14)$$

Therefore, the initial event site for non-convex regions can be selected in the following manner:

1. Select an isotropic direction.

2. Save all boundary positions encountered by a ray from $\bar{r}$ in the selected direction. (These boundary positions are indexed sequentially as encountered; there is an odd number of boundary positions for all closed surfaces.)

3. Select, with equal probability, the initial event site from the saved boundary positions.

4. If the index of the selected boundary position is even, set the statistical weight of the "walker" negative; otherwise, set it positive.

Selection of subsequent event sites is performed in a similar manner.

Consider now the following particle transport analogy to obtain a Monte Carlo solution to Equations (7) and (8) for convex regions:

1. λ is set to 0.0.

2. A particle isotropically emitted from $\bar{r}$ strikes the surface at $\bar{r}_{so}$.

3. $Q(\bar{r}_{so})$ is added to λ.

4. The particle is reflected isotropically and strikes the surface again at $\bar{r}_{s1}$.

5. $Q(\bar{r}_{s1})$ is subtracted from λ.

6. The particle is reflected isotropically and strikes the surface again at $\bar{r}_{s2}$.

7. $Q(\bar{r}_{s2})$ is added to λ.

.
.
.

ad infinitum.

The logic of the above random walk (other than the "ad infinitum") is easily adaptable to current Monte Carlo radiation-transport codes. Particles are simply reflected isotropically from the inner surface of the region. The calculation depicts particles trapped in an internal void that is surrounded by a perfectly elastic, isotropic, albedo surface.

The non-termination of the random walk represents the divergence of the Neumann series approximation to Equations (7) and (8). This series can be written as

$$T(\bar{r}) = \lim_{N\to\infty} \sum_{n=0}^{N} \int d\bar{r}_s \; Q(\bar{r}_s) \; \mu_n^* \; (\bar{r}_s), \tag{15}$$

where

$$\mu_o^* \; (\bar{r}_s) = R(\bar{r},\bar{r}_s)$$

$$\mu_n^* \; (\bar{r}_s) = -\int d\bar{r}_p \; \mu_{n-1}^*(\bar{r}_p) \left| K(\bar{r}_s,\bar{r}_p) \right| \; . \tag{16}$$

The limit in Equation (15) does not exist, as can be illustrated in heat transfer. The temperature, $\phi(\bar{r}_s)$, on the surface of a homogeneous solid is given, and the temperature, $T(\bar{r})$, at a point, $\bar{r}_o$, within the solid is desired. Terms in the Neumann series, Equation (15), can be calculated with Monte Carlo methods as follows:

1. A large number of particles, m, are emitted isotropically from $\bar{r}_o$. The temperatures at the points these particles strike the surface [$\phi(\bar{r}_{s1})$, $\phi(\bar{r}_{s2}),\ldots,\phi(\bar{r}_{sm})$] are added, multiplied by 2.0, and divided by m. This quantity, say T_o, is an estimate of the first term in Equation (15).

2. These m particles are re-emitted isotropically from their impact points. Again the surface temperatures at the new impact points are added, multiplied by 2.0, and divided by m to obtain T_1. The first two terms in the series of Equation (15) are T_o and $-T_1$.

3. This process is repeated N times. The series can now be approximated as

$$T(\bar{r}_o) \cong \sum_{n=0}^{N} (-1)^n T_n \; . \tag{17}$$

4. Eventually the m particles will attain an equilibrium (eigenfunction) distribution, independent of $\bar{r}_o$. Then the expectation value of T_n will equal the expectation value of T_{n+1}, say T_e. Therefore, the series of Equation (17), and hence Equation (15), will have oscillations of $\pm T_e$; i.e., the limit does not exist.

Although the Neumann series does not converge for Equations (7) and (8), it can be shown that solutions to these equations do exist and are unique[11,12]. The Neumann series is not the most general solution to the Fredholm equation, i.e., there are Fredholm equations that have solutions, Equation (8) being an example, and yet these solutions cannot be expressed as a Neumann series. A series can be generated for the Fredholm integral equation as follows:

$$T(\bar{r}) = \lim_{N\to\infty} \sum_{n=0}^{N} \int d\bar{r}_s \; Q(\bar{r}_s) \; \mu_n^*(\bar{r}_s), \tag{18}$$

where

$$\mu_o^*(\bar{r}_s) = R(\bar{r},\bar{r}_s) - \tfrac{1}{2} \int d\bar{r}_p \; R(\bar{r},\bar{r}_p)|K(\bar{r}_s,\bar{r}_p)|$$

$$\mu_1^*(\bar{r}_s) = -\tfrac{1}{2}\left[\int d\bar{r}_p \; R(\bar{r},\bar{r}_p)|K(\bar{r}_s,\bar{r}_p)| - \int d\bar{r}_p \int d\bar{r}_t R(\bar{r},\bar{r}_p) \; X \right.$$

$$\left. |K(\bar{r}_t,\bar{r}_p)||K(\bar{r}_s,\bar{r}_t)|\right] \tag{19}$$

$$\mu_n^*(\bar{r}_s) = -\int d\bar{r}_p \; \mu_{n-1}^*(\bar{r}_p)|K(\bar{r}_s,\bar{r}_p)| \quad \text{for } n > 1.$$

This series can be shown to converge to the solution of Equation (18) by the alternating series test. Implementation of the above solution in radiation codes requires changes in the logic used for the Neumann solution to terminate histories.

The proposed method, as outlined above, appears at first glance to be useful for the calculation of $T(\bar{r})$ at only one point at a time. However, $T(\bar{r})$ can be calculated at many positions simultaneously, with only a small increase in computational time, by using statistical weights. For example, if $T(\bar{r})$ is desired at $\bar{r}_1$ and $\bar{r}_2$, the initial event can be selected by starting a particle isotropically from $\bar{r}_1$. Contributions for $\bar{r}_2$ are then multiplied (weighted) by

$$\frac{R(\bar{r}_2,\bar{r}_s)}{R(\bar{r}_1,\bar{r}_s)} = \frac{[(\bar{r}_2 - \bar{r}_s)\cdot\hat{n}_s]\;[(\bar{r}_1 - \bar{r}_s|^3]}{[(\bar{r}_1 - \bar{r}_s)\cdot\hat{n}_s]\;[|\bar{r}_2 - \bar{r}_s|^3]}, \tag{20}$$

where $\bar{r}_s$ is the site of the initial event. This weighting is justified because once a particle strikes the surface at a given point, the random walk is independent of its origin. This weighting is a highly

useful property of the surface density technique. With Equation (20) the temperature at any number of points (temperature distributions) can be calculated from one set of Monte Carlo histories. The temperature differences (or gradients) calculated in this correlated fashion are more meaningful than those from independent histories.

3.2 Pictorial Demonstration.

The surface density method is illustrated in Figure 4.

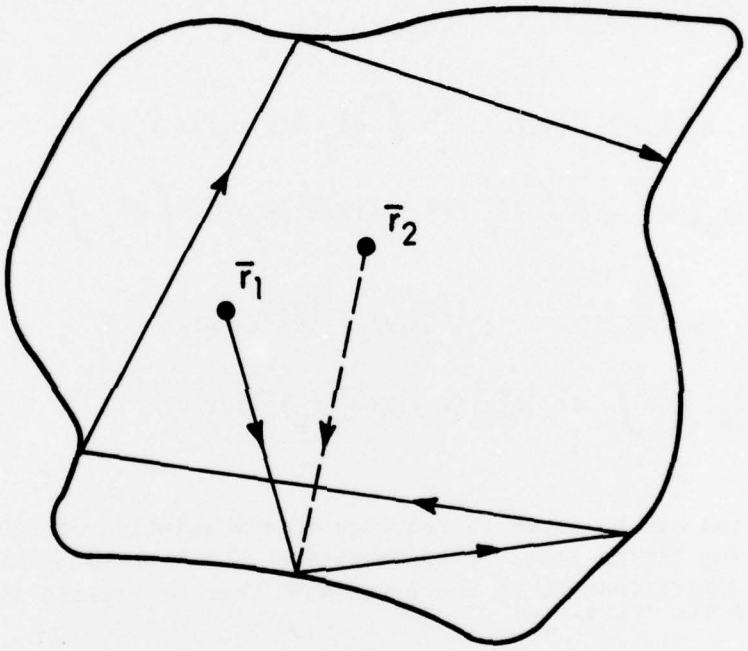

Figure 4. Surface Density Approach to the Dirichlet Problem.

A walker starts at the point where the temperature is desired, $\bar{r}_1$ in Figure 4. It leaves this point isotropically and moves directly to the surface with no intermediate steps. The temperature at the surface point encountered by the walker is saved. The walker then moves from this surface point, isotropically-inward, directly to another surface point. The walk is continued until four or five surface temperatures are collected. These temperatures are combined in a series (Equation (18)), and this combined temperature is a Monte Carlo estimate of the temperature at $\bar{r}_1$. Since the series for the Fredholm equation is truncated, i.e., only four or five surface temperatures are used, a numerical approximation results. The truncation error can be estimated from the last calculated term of the series. The

temperature at $\bar{r}_2$ in Figure 4 can be obtained by weighting each history from $\bar{r}_1$ using Equation (20).

4. APPLICATIONS

4.1 Two-Dimensional Convex Regions.

The Monte Carlo radiation transport code MORSE[17] was altered to provide isotropic reflection at albedo surfaces, to calculate the terms of the series (see Equation (18)), and to weight the detector positions (see Equation (20)). Since the first problem is two-dimensional, it requires a slight modification to Equations (8) and (20). The modified two-dimensional forms are listed below for reference:

$$\mu^*(\bar{r}_s) = \frac{(\bar{r}-\bar{r}_s)\cdot\hat{n}_s}{2\pi|\bar{r}-\bar{r}_s|^2} + \int \frac{(\bar{r}_s-\bar{r}_p)\cdot\hat{n}_s}{\pi|\bar{r}_s-\bar{r}_p|^2}\ \mu^*(\bar{r}_p)d\bar{r}_p\ , \qquad (8a)$$

$$\frac{R(\bar{r}_2,\bar{r}_s)}{R(\bar{r}_1,\bar{r}_s)} = \frac{[(\bar{r}_2-\bar{r}_s)\cdot\hat{n}_s][|\bar{r}_1-\bar{r}_s|^2]}{[(\bar{r}_1-\bar{r}_s)\cdot\hat{n}_s][|\bar{r}_2-\bar{r}_s|^2]}\ . \qquad (20a)$$

We require the temperature at various points within a square situated in the region $0 \leq x \leq 1$, $0 \leq y \leq 1$. The surface temperature is unity on the side $x = 0$, $0 \leq y \leq 1$ and zero on the other boundaries. Separation of variables provides the analytic solution,

$$T(x,y) = \frac{4}{\pi}\sum_{n=0}^{\infty} \frac{\sinh[(2n+1)\pi(1-x)]\ \sin[(2n+1)\pi\ y]}{(2n+1)\sinh[(2n+1)\pi]}\ . \qquad (21)$$

Temperatures were calculated at nine (detector) positions with the initial (source) position determined by random selection. The Monte Carlo results, along with the corresponding analytic results, are shown in Table I. This run of 10,000 histories required 17 s of CPU time on the CDC 7600. An identical calculation for only one detector required 12 s.

---

17. E.A. Straker, N.R. Byrn and W.H. Scott, Jr., "The MORSE Code With Combinatorial Geometry", SAI-72-511-LJ, Science Applications, Inc., (1972).

TABLE I. RESULTS OF TWO DIMENSIONAL CALCULATION[a]

DETECTOR	POSITION (x,y)	ANALYTIC	MONTE CARLO
1	(.25, .25)	0.43	0.43 ± 0.03
2	(.25, .50)	0.54	0.54 ± 0.03
3	(.25, .75)	0.43	0.45 ± 0.03
4	(.50, .25)	0.18	0.20 ± 0.02
5	(.50, .50)	0.25	0.26 ± 0.02
6	(.50, .75)	0.18	0.19 ± 0.03
7	(.75, .25)	0.07	0.08 ± 0.02
8	(.75, .50)	0.10	0.11 ± 0.02
9	(.75, .75)	0.07	0.08 ± 0.02

(a) These Monte Carlo results were obtained in one run of 10,000 histories which required 17 s of CPU time on the CDC 7600; temperatures for the nine detectors were obtained simultaneously by the weighting technique (Equation 20a).

4.2 Three-Dimensional Convex Regions.

The second problem treats a finite cylinder with height and radius both equal to 6 metres. The outer surface of the cylinder is at 400°C with the top and bottom surfaces at 100 and 300°C, respectively. The analytic solution is given by the following expression[18]:

$$T(r,z) = 100 \sum_{n=1}^{\infty} \left\{ \frac{J_o(r\alpha_n)}{\alpha_n J_1(6\alpha_n)\sinh(6\alpha_n)} \left[\sinh(6-z)\alpha_n + \frac{\sinh \alpha_n z}{3} \right] + \frac{16}{\pi} \frac{I_o[(2n-1)\pi r/6]}{(2n-1) I_o[2n-1)\pi]} \sin \frac{(2n-1)\pi z}{6} \right\}, \quad (22)$$

where α_n are the roots of the Bessel functions.

18. H.S. Carslaw and J.C. Jaeger, Conduction of Heat in Solids, Oxford at the Clarendon Press, 2nd ed. New York, NY (1959).

Temperatures were calculated at ten positions with the source weighting of Equation (20). The analytical and Monte Carlo results are compared in Figure 5.

4.3 Three-Dimensional Non-Convex Regions.

The third problem treats a region with both concave and convex surfaces, viz., a finite hollow cylinder (Figure 6). MORSE was modified to generate secondary particles at the surface of the region. These secondary particles were given positive or negative statistical weights in accordance with the algorithm that follows Equation (14). The Monte Carlo results from MORSE and the analytical results from Carslaw and Jaeger (18) in Table II.

TABLE II. RESULTS FOR FINITE HOLLOW CYLINDER PROBLEM.

R	Z	M.C.[a]	Analytic
5.0	5.0	134°C ± 11°C	134°C
5.0	4.0	141°C ± 7°C	142°C
5.5	3.0	123°C ± 5°C	121°C
5.0	3.0	141°C ± 4°C	144°C
4.5	3.0	164°C ± 6°C	174°C

[a]These Monte Carlo results were obtained with one run of 10,000 histories which required 2.04 min of CPU time on the CDC 7600.

Three independent calculations were made for this problem. The first case, for a single temperature, required 1.80 min on the CDC 7600; the second, for two temperatures, 1.87 min. The third calculation, for the temperatures at the five positions shown in Table II, required 2.04 min of computer time. These times demonstrate the advantages of the weighting technique, Equation (20).

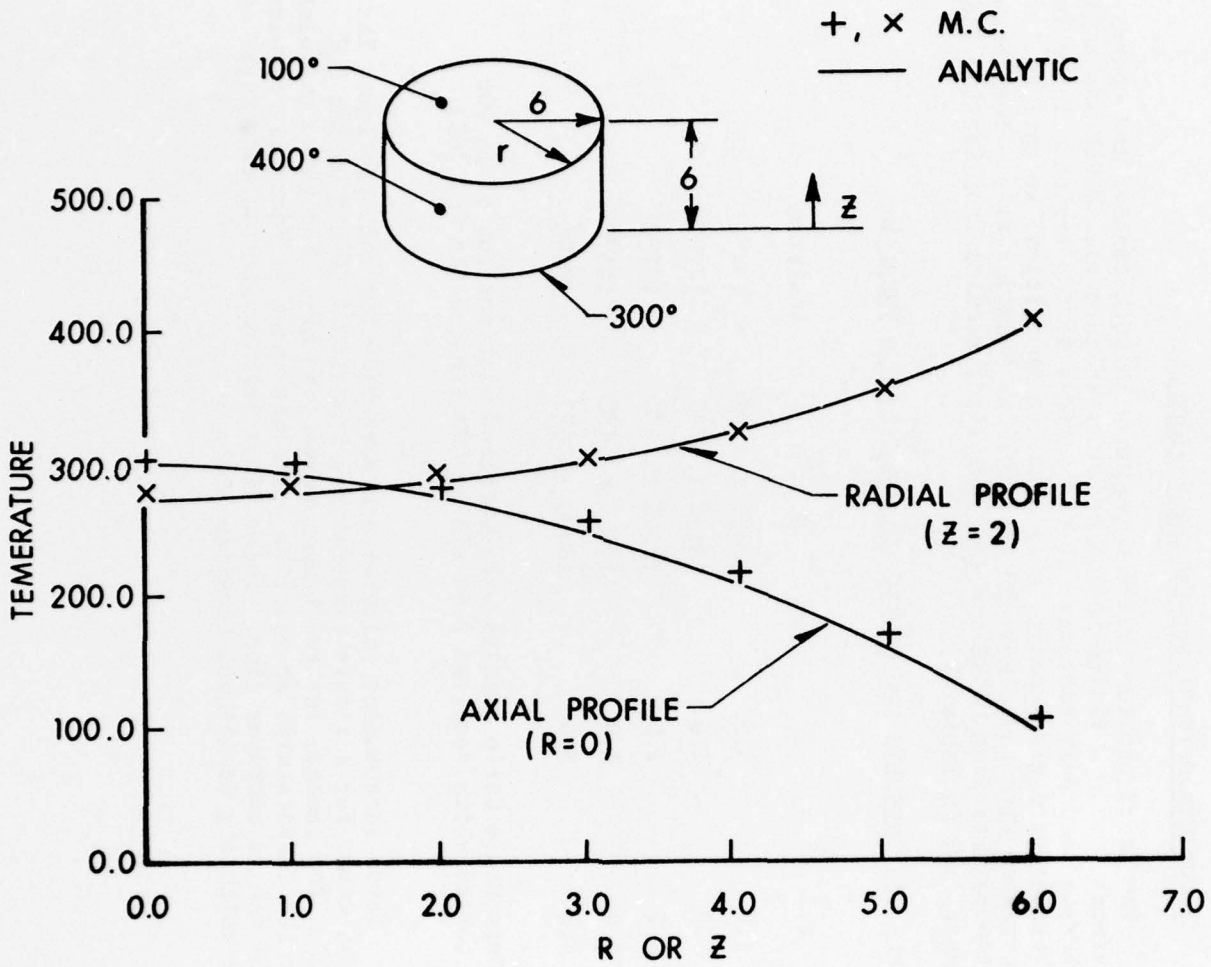

Figure 5. Results for Solid Cylinder Calculation.

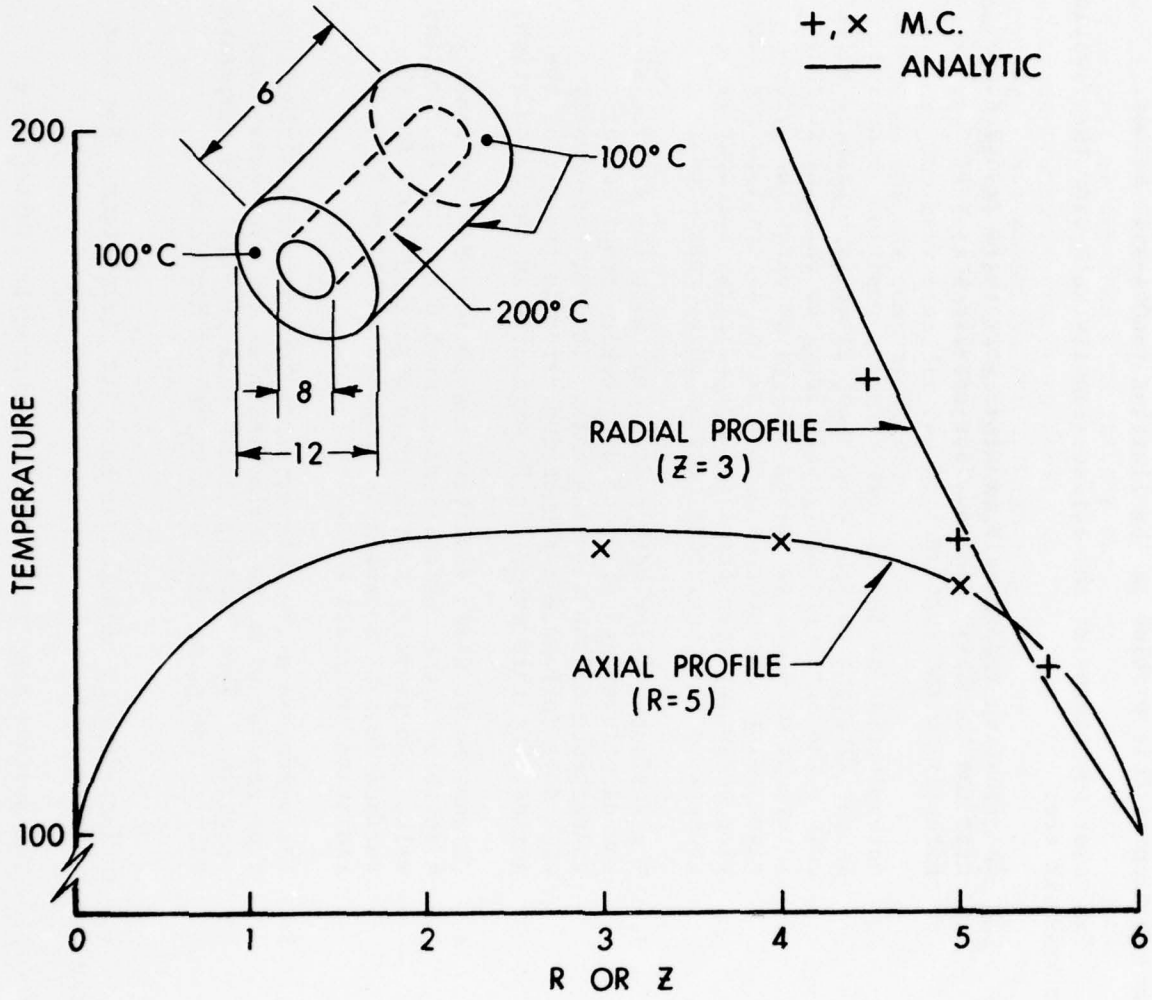

Figure 6. Geometry and Boundary Conditions for Finite Hollow Cylinder.

5. SUMMARY

The surface-density technique is a continuous Monte Carlo method for the solution of the Dirichlet heat transfer problem. The only other continuous Monte Carlo method that allows large random steps in the solution to this problem is the floating random-walk method.

The major advantages of the surface-density walk over the floating random-walk are:

1. The floating random walk required very small random steps near the boundary. The surface-density walk proceeds directly to the surface.

2. Determination of the closest boundary position (required in the floating walk at each event site) is extremely difficult. The surface density walk requires only the surface intercept of a walker moving in a given direction from a given point. Geometry searches of the latter type are less time consuming even for simple geometries; for complex geometries this advantage becomes more pronounced.

3. The surface-density method does away with the artificial boundary layer and its attendant errors required for convergence of the floating walk. The surface-density walk does introduce a truncation error in evaluating the series, but this error can be estimated in the calculation.

4. Current Monte Carlo radiation transport codes are readily adaptable to the surface-density method but not to floating walk. The geometry search logic described above for the surface-density approach is standard in all Monte Carlo radiation transport codes.

5. The surface-density walk provides temperature distributions from one set of Monte Carlo histories through statistical weighting. The floating random walk provides the temperature only at one point with a given set of histories.

The surface-density method does have its limitations. For heat transfer these include:

1. The surface density approach is currently limited to a single medium.

2. The type of boundary condition determines the integral formulation, i.e., Equations (7) and (8). Therefore different types of boundary conditions, e.g., convective boundary conditions, require the simulation of different integral equations.

3. The surface-density Monte Carlo approach as formulated in this paper is applicable only to time-independent problems.

These limitations severely restrict the applicability of the surface-density Monte Carlo technique. However, these limitations can perhaps be overcome with further development. Since the surface-density Monte Carlo approach is readily incorporated in Monte Carlo radiation transport codes, we feel that such development is worth pursuing. This compatibility is highly useful for the many problems that require calculations of both heat transfer and radiation transport. If this compatibility can be maintained, then criticality, shielding, and heat transfer can be calculated with one geometric description and one computer code.

This method should be applied to heat transfer and boundary layer analyses in problems of interior ballistics. The aspect of a boundary layer being physically a single medium transport phenomenon makes this approach extremely attractive. Also, making use of this technique would allow the boundary layer analysis and the heat transport processes to be simulated by a single computer code without recourse to gross simplifying assumptions which are usually made in the solution to boundary layer problems.

REFERENCES

1. E.S. Troubetzkoy et al, "Solution of Time Dependent Diffusion Equation in Complex Geometry by the Monte Carlo Method", BRL Interim Technical Report, MAGI 7053 (Rough Draft) 1975.

2. T.J. Hoffman and N.E. Banks, "Monte Carlo Solution to the Dirichlet Problem With the Double Layer Potential Density", Trans. Am. Nucl. Soc., 18, 136 (1974).

3. N.E. Banks and T.J. Hoffman, "Continuous Monte Carlo Solution to the Dirichlet Heat Transfer Problem Using the Double Layer Potential", 20th Army Mathematics Conference, Boston, MA 1974.

4. T.J. Hoffman and N.E. Banks, "Monte Carlo Solution to the Dirichlet Problem", Transactions of the ANL-NEACRP International Meeting on Monte Carlo Applications, Argonne National Laboratory, July 1-3, 1974.

5. J.H. Curtiss, "Sampling Methods Applied to Differential and Difference Equations", Seminar on Scientific Computation, International Business Machines Corporation 1949.

6. G.M. Brown, "Monte Carlo Methods", Modern Mathematics for the Engineer, McGraw-Hill Book Co., Inc., New York, NY 1956.

7. A. Haji Sheikh and E.M. Sparrow, "The Solution of Heat Conduction Problems by Probability Methods", J. Heat Transfer, ASME, 89, 1967.

8. A. Haji-Sheikh and E.M. Sparrow, "The Floating Random Walk and Its Application to Monte Carlo Solutions of Heat Equations", J. SIAM, Appl. Math., 14, 1966.

9. M.E. Muller, "Some Continuous Monte Carlo Methods for the Dirichlet Problem", Annals of Math. Statistics, 27, 1956.

10. M.H. Kalos and H. Steinberg, private communications at the ANL-NEACRP International Meeting on Monte Carlo Applications, Argonne National Laboratory, July 1-3, 1974.

11. S.G. Mikhlin, Linear Integral Equations, Hindustan Publishing Corporation, Delhi, India 1960.

12. W.V. Lovitt, Linear Integral Equations, Dover Publications, Inc., New York, NY 1950.

13. T.W. Armstrong and P.N. Stevens, "A V^{O} Importance Function for the Monte Carlo Calculation of the Deep Penetration of Gamma Rays", Pergamon Press, New York, NY 1969.

14. H. Kahn, "Applications of Monte Carlo", Part II, AECU-3259, Rand Corporation, Santa Monica, CA 1956.

15. R.R. Coveyou, V.R. Cain and K.J. Yost, "Adjoint and Importance in Monte Carlo Applications", NSE, 27 1967.

16. W. Kaplan, Advanced Calculus, Addison-Wesley Pub. Co., Inc., Reading, MA 1959.

17. E.A. Straker, N.R. Byrn and W.H. Scott, Jr., "The MORSE Code With Combinatorial Geometry", SAI-72-511-LJ, Science Applications, Inc., 1972.

18. H. S. Carslaw and J.C. Jaeger, Conduction of Heat in Solids, Oxford at the Clarendon Press, 2nd ed. New York, NY 1959.

DISTRIBUTION LIST

No. of Copies	Organization
12	Commander Defense Documentation Center ATTN: DDC-TCA Cameron Station Alexandria, VA 22314
1	Director Defense Nuclear Agency ATTN: RATN Washington, DC 20305
1	Commander US Army Materiel Development and Readiness Command ATTN: DRCDMA-ST 5001 Eisenhower Avenue Alexandria, VA 22333
1	Commander US Army Aviation Systems Command ATTN: DRSAV-E 12th and Spruce Streets St. Louis, MO 63166
1	Director US Army Air Mobility Research and Development Laboratory Ames Research Center Moffett Field, CA 94035
1	Commander US Army Electronics Command ATTN: DRSEL-RD Fort Monmouth, NJ 07703
1	Commander US Army Missile Research and Development Command ATTN: DRDMI-R Redstone Arsenal, AL 35809
1	Commander US Army Tank-Automotive Development Command ATTN: DRDTA-RWL Warren, MI 48090
2	Commander US Army Mobility Equipment Research & Development Command ATTN: Tech Docu Cen, Bldg. 315 DRSME-RZT Fort Belvoir, VA 22060
1	Commander US Army Armament Materiel Readiness Command Rock Island, IL 61202
1	Commander US Army Frankford Arsenal ATTN: SARFA-FCV, Stan Goodman Philadelphia, PA 19137
2	Commander US Army Picatinny Arsenal ATTN: SARPA-ND-C-T JAWTIP/SARPA-RT-S Dover, NJ 07801
1	Commander US Army Harry Diamond Labs ATTN: DRXDO-TI 2800 Powder Mill Road Adelphi, MD 20783
1	Director US Army TRADOC Systems Analysis Activity ATTN: ATAA-SA White Sands Missile Range NM 88002
1	Commander US Army Nuclear Agency Fort Bliss, TX 79916
1	AFWL (SUL) Kirtland AFB, NM 87117

DISTRIBUTION LIST (CONT'D)

No. of Copies	Organization
1	Director Lawrence Livermore Laboratory ATTN: Tech Info Div P.O. Box 808 Livermore, CA 94550
1	Director Los Alamos Scientific Laboratory ATTN: Rept Lib P.O. Box 1663 Los Alamos, NM 87544
1	Radiation Schielding Info Ctr Bldg 6025, P.O. Box X Oak Ridge National Laboratory Oak Ridge, TN 37830
1	Science Applications, Inc. ATTN: Dr. Dave Sargis 1200 Prospect Place P.O. Box 2351 La Jolla, CA 92037
1	Science Applications, Inc. Suite 800 ATTN: Mr. Ronnie Guy 2109 W. Clinton Bldg Huntsville, AL 35805
1	Science Applications, Inc. ATTN: Dr. Pete Versteegen 8400 Westpark Drive Mclean, VA 22101
2	MAGI ATTN: Drs. Trnbetskoy/Kalds 3 Westchester plaza Elmsford, NY 10523
	Aberdeen Proving Ground
	Marine Corps Ln Ofc Dir, USAMSAA